Measurement report: Oxidation potential of water-soluble aerosol components in the southern and northern of Beijing

Wei Yuan[1], Ru-Jin Huang[1], Chao Luo[2], Lu Yang[1], Wenjuan Cao[1], Jie Guo[1], Huinan Yang[2]

[1]State Key Laboratory of Loess and Quaternary Geology, Center for Excellence in Quaternary Science and Global Change, Institute of Earth Environment, Chinese Academy of Sciences, Xi'an 710061, China.

[2]School of Energy and Power Engineering, University of Shanghai for Science and Technology, Shanghai 200093, China

Correspondence: Ru-Jin Huang (rujin.huang@ieecas.cn) and Huinan Yang (yanghuinan@usst.edu.cn)

Abstract

Water-soluble components have significant contribution to the oxidative potential (OP) of atmospheric fine particles (PM$_{2.5}$), while our understanding of water-soluble PM$_{2.5}$ OP and its sources, as well as its relationship with water-soluble components, is still limited. In this study, the water-soluble OP levels in wintertime PM$_{2.5}$ in the south and north of Beijing, representing the difference in sources, were measured with dithiothreitol (DTT) assay. The volume normalized DTT (DTT$_v$) in the north (3.5 ± 1.2 nmol min^{-1} m^{-3}) was comparable to that in the south (3.9 ± 0.9 nmol min^{-1} m^{-3}), while the mass normalized DTT (DTT$_m$) in the north (65 ± 28 pmol min^{-1} μg^{-3}) was almost twice that in the south (36 ± 14 pmol min^{-1} μg^{-3}). In both the south and north of Beijing, DTT$_v$ was better correlated with soluble elements instead of total elements. In the north, soluble elements (mainly Mn, Co, Ni, Zn, As, Cd and Pb) and water-soluble organic compounds, especially light-absorbing compounds (also known as brown carbon), had positive correlations with DTT$_v$. However, in the south, the

29   DTT_v was mainly related to soluble As, Fe and Pb. The sources of DTT_v were further

30   resolved using the positive matrix factorization (PMF) model. Traffic-related

31   emissions (39%) and biomass burning (25%) were the main sources of DTT_v in the

32   south, and traffic-related emissions (> 50%) contributed the most of DTT_v in the north.

33   Our results indicate that vehicle emission was the important contributor to OP in

34   Beijing ambient $PM_{2.5}$ and suggest that more study is needed to understand the

35   intrinsic relationship between OP and light absorbing organic compounds.

36

37   **1 Introduction**

38   Atmospheric fine particulate matter ($PM_{2.5}$) pollution is one of the major global

39   environmental issues, affecting air quality, climate and human health (Huang et al.,

40   2014; Burnett et al., 2018; An et al., 2019; Zheng et al., 2020). The exposure to $PM_{2.5}$

41   was estimated to be responsible for 8.9 million deaths worldwide in 2015, of which

42   28% occurred in China (Burnett et al., 2018). Numerous studies have shown that

43   oxidative stress is one possible mechanisms underlying the adverse effects of $PM_{2.5}$

44   on human health (Chowdhury et al., 2019; Lelieveld et al., 2021; Yu et al., 2022b;

45   Guascito et al., 2023). When entering the human body, $PM_{2.5}$ can induce the

46   production of excessive reactive oxygen species (ROS) (e.g., H_2O_2, $\cdot OH$ and $\cdot O_2^-$),

47   leading to cellular redox imbalance and generating oxidative stress effects. The ability

48   of $PM_{2.5}$ to cause oxidative stress is defined as oxidative potential (OP).

49   The methods to determine the OP of $PM_{2.5}$ include cellular and acellular assays,

50   and acellular methods are more widely used than cellular methods (Charrier and

51   Anastasio, 2012; Xiong et al., 2017; Calas et al., 2018; Bates et al., 2019; Wang et al.,

52   2020b; Campbell et al., 2021; Oh et al., 2023). Among acellular methods, the

53   dithiothreitol (DTT) assay is extensively applied to determine the OP of ambient

54   particles (Charrier and Anastasio, 2012; Xiong et al., 2017; Liu et al., 2018; Wang et

55   al., 2020b; Puthussery et al., 2022; Wu et al., 2022a). DTT is a surrogate of cellular

56   reductants, and the consumption rate of DTT was used to assess the OP of $PM_{2.5}$.

57   Previous studies have shown that organic matters (e.g., water-soluble organic species

and PAHs) and some transition metals (e.g., Mn and Cu) are the important contributors to DTT consumption of $PM_{2.5}$ (Charrier and Anastasio, 2012; Verma et al., 2015; Bates et al., 2019; Wu et al., 2022a; Wu et al., 2022b). For example, Charrier and Anastasio (2012) measured the OP of $PM_{2.5}$ in San Joaquin Valley, California and reported that about 80% of DTT consumption was contributed by transition metals. Verma et al. (2015) measured the OP of water-soluble $PM_{2.5}$ in the southeastern United States and reported that about 60% of DTT activity was contributed by water-soluble organics. The mixtures of metals and organics may produce synergistic or antagonistic effects, such as $\cdot O_2^-$ produced from oxidation of DTT by quinones is more efficiently transformed to $\cdot OH$ in the presence of Fe, while the DTT consumption and $\cdot OH$ generation of quinones are reduced in the presence of Cu (Xiong et al., 2017; Yu et al., 2018; Bates et al., 2019).

A number of studies have investigated the OP of water-soluble components in $PM_{2.5}$, which show that the average water-soluble OP values in urban areas ranged from 0.1 to 10 nmol min^{-1} m^{-3} (Fang et al., 2016; Liu et al., 2018; Chen et al., 2019; Wu et al., 2022a; Yu et al., 2022a; Xing et al., 2023). Due to the complexity in chemical composition and sources of $PM_{2.5}$ that determine the OP levels, the sources of OP are also diverse (Verma et al., 2015; Bates et al., 2019; Tuet et al., 2019; Yu et al., 2019; Cao et al., 2021). Several studies have investigated the emission sources and ambient samples to identify the sources of OP (Tuet et al., 2019; Yu et al., 2019; Wang et al., 2020b; Cao et al., 2021), which include both primary and secondary sources. For example, Cao et al. (2021) measured the water-soluble OP of $PM_{2.5}$ samples from six biomass and five coal burning emissions in China, with average values of 4.5-7.4 and 0.5-2.1 pmol min^{-1} μg^{-1}, respectively. Tong et al. (2018) investigated the OP of secondary organic aerosols (SOA) from oxidation of naphthalene, isoprene and β-pinene with $\cdot OH$ or O_3, which were 104 ± 7.6, 48 ± 7.9 and 36 ± 3.1 pmol min^{-1} μg^{-1}, respectively. Verma et al. (2014) identified the sources of water-soluble OP of $PM_{2.5}$ in Atlanta, United States from June 2012 to September 2013 with positive matrix factorization (PMF) and chemical mass balance (CMB) methods, of which biomass

burning was the largest contributor. Wang et al. (2020b) quantified the sources of water-soluble OP of $PM_{2.5}$ in Xi'an, China in 2017 using PMF and multiple linear regression (MLR) methods, with significant contributions from secondary sulfates, vehicle emissions and coal combustion. Some studies have also measured the OP of particles with different particle sizes, and reported that smaller size fractions typically have higher ROS activity compared to large PM size fractions (Saffari et al., 2014; Shafer et al., 2016; Besis et al., 2023). For example, Besis et al. (2023) measured the OP of water-soluble fraction of size segregated PM (< 0.49, 0.49-0.95, 0.95-1.5, 1.5-3.0, 3.0-7.2 and > 7.2 μm) collected during the cold and warm periods at an urban site in Thessaloniki, northern Greece, and the results showed that the total DTT activity of the PM < 3 μm size fraction were higher (2-5 times) than that of PM > 3 μm size fraction in both warm and cold periods. Despite these efforts, comparative studies on the differences in pollution levels and sources of $PM_{2.5}$ OP in different districts are still limited.

In this study, the DTT activity of water-soluble matter in $PM_{2.5}$ samples collected simultaneously in the southern and northern of Beijing in January 2018 were measured. The concentration and light absorption of water-soluble organic carbon (WSOC), as well as the concentrations of 14 trace elements and 7 light-absorbing nitroaromatic compounds (NACs) were quantified. The sources of DTT activity were then identified with PMF model. The results acquired in this study provide a comparison of $PM_{2.5}$ OP in different districts of Beijing and its connection with organic compounds, trace elements and sources, which could be helpful for further study of the regional differences in the effects of $PM_{2.5}$ on human health.

2 Materials and methods

2.1 Sampling

Ambient 24 h integrated $PM_{2.5}$ filter samples were collected from January 1 to 31, 2018 simultaneously in the south (the Dingfuzhuang village (DFZ), Daxing district; 39.61°N, 116.28°E) and north (the National Center for Nanoscience and Technology

(NCNT), Haidian district; 39.99°N, 116.32°E) of Beijing (Figure S1). The distance between the two sampling sites is about 42 km. The south site is surrounded by agricultural, industrial, and transportation areas, and the north site is surrounded by residential, transportation and commercial areas. $PM_{2.5}$ samples were collected on pre-baked (780 °C, 3 h) quartz-fiber filters (20.3 × 25.4 cm; Whatman, QM-A, Clifton, NJ, USA) using high-volume $PM_{2.5}$ samplers (1.13 m^{-3} min^{-1}; Tisch, Cleveland, OH, USA) which were placed on the roof of buildings at heights of about 5 m (south) and 20 m (north) above the ground. 31 samples were collected at each site. After collection, the samples were wrapped in baked aluminum foils and stored in a freezer (−20 °C) until further analysis.

2.2 Chemical analysis

The mass of $PM_{2.5}$ on the filter was measured by a digital microbalance with a precision of 0.1 mg (LA130S-F, Sartorius, Germany) after 24-h equilibration at a constant temperature (20-23 °C) and humidity (35-45%) chamber. Each filter was weighted at least two times, and the deviations for blank and sampled filters among the repetitions were less than 5 and 10 μg, respectively. The $PM_{2.5}$ mass concentration was calculated by dividing the weight difference before and after sampling by the volume of sampled air.

For WSOC analysis, one punch (1.5 cm^2 for concentration analysis and 0.526 cm^2 for light absorption measurement) of filter was taken from each sample and extracted ultrasonically with ultrapure water (> 18.2 MΩ cm) for 30 min. After, the extracts were filtered with a 0.45 μm PVDF pore syring filter to remove insoluble substances. Finally, the concentration of WSOC was measured with a total organic carbon-total nitrogen analyzer (TOC-L, Shimadzu, Japan; (Ho et al., 2015)) and the light absorption of WSOC was measured by an UV-Vis spectrophotometer (300-700 nm; Ocean Optics, USA) equipped with a liquid waveguide capillary cell (LWCC-3100, World Precision Instruments, Sarasota, FL, USA; (Yuan et al., 2020)). The absorption coefficient (Abs) of WSOC was calculated according to formula S1 in the Supporting Information (SI).

The total concentration and soluble fraction concentration of 14 trace elements (i.e., Ti, V, Cr, Mn, Fe, Co, Ni, Cu, Zn, As, Sr, Cd, Ba, and Pb) were quantified by an inductively coupled plasma mass spectrometer (ICP-MS, 7700x, Agilent Technologies, USA), and the details are shown in the SI. For soluble fraction concentration analysis, a punch of filter (47 mm diameter) was extracted with ultrapure water and then centrifuged from residues. For total concentration analysis, another 47 mm diameter filter of the same sample was used and digested with 10 mL HNO_3 and 1 mL HF at 180 °C for 12 h. The extracts were then heated and concentrated to ~ 0.1 mL, and diluted to 5 mL with 2% HNO_3. Afterwards, the diluents were filtered with a 0.22 μm PTFE pore syring filter and stored in a freezer (−4 °C) until further ICP-MS analysis.

The concentrations of organic markers (including levoglucosan, mannosan, galactosan, hopanes (including 17α(H)-22,29,30-trisnorhopane, 17α(H),21β(H)-30-norhopane, 17β(H),21α(H)-30-norhopane, 17β(H),21α(H)-hopane, 17β(H),21α(H)-hopane and 17β(H),21α(H)-hopane), picene, phthalic acid, isophthalic acid and terephthalic acid) and light-absorbing NACs (including 4-nitrophenol (4NP), 2-methyl-4-nitrophenol (2M4NP), 3-methyl-4-nitrophenol (3M4NP), 4-nitrocatechol (4NC), 3-methyl-5-nitrocatechol (3M5NC), 4-methyl-5-nitrocatechol (4M5NC) and 4-nitro-1-naphthol (4N1N)) were determined by a gas chromatograph–mass spectrometer (GC-MS; Agilent Technologies, Santa Clara, CA, USA) following the method described elsewhere (Wang et al., 2020a), and more details about the analysis can be found in SI. All of the results reported in this study were corrected for blanks.

2.3 Oxidative potential

The DTT assay was applied to determine the oxidative potential of water-soluble components in $PM_{2.5}$ according to the method by Gao et al. (2017). In brief, a quarter of a 47 mm filter was ultrasonically extracted with 5 mL ultrapure water for 30 min and then filtered with a 0.45 μm PVDF pore syring filter to remove insoluble substances. Several studies have shown that ultrasonic treatment of samples can lead to an increase in their OP values (Miljevic et al., 2014; Jiang et al., 2019), however, there was also a study showed that the difference in OP values of water-soluble $PM_{2.5}$

174 measured by DTT assay was small for samples extracted by ultrasonic and shaking

175 (Gao et al., 2017). Consistent with the extraction methods for organic markers and

176 trace elements, ultrasonic method was used to extract samples for DTT analysis.

177 Afterwards, 0.5 mL of the extract was mixed with 1 mL of potassium phosphate

178 buffer (pH = 7.4) and 0.5 mL of 2 mM DTT in a brown vial, and then placed in a

179 water bath at 37 °C. Then, 20 μL of this mixture was taken at designated time

180 intervals (2, 7, 13, 20, and 28 min) and mixed with 1 mL trichloroacetic acid (TCA;

181 1% w/v) in another brown vial to terminate the reaction. Then, 0.5 mL of 5,5'-

182 dithiobis-(2-nitrobenzoic acid) (DTNB; 2.5 μM) and 2 mL of tris buffer (pH = 8.9)

183 were added to form 2-nitro-5-thiobenzonic acid (TNB) which has light absorption at

184 412 nm. Finally, the absorption of TNB was measured by a LWCC-UV-Vis. The DTT

185 consumption rate was quantified by the remaining DTT concentration at different

186 reaction times. Daily solution blanks and filter blanks were analyzed in parallel with

187 samples to evaluate the consistency of the system performance. Besides, for every 10

188 samples, one sample was chosen to be measured three times to check the

189 reproducibility, and the relative standard deviation was lower than 5%. Ambient

190 samples were corrected for filter blank. The DTT activities were normalized by the

191 volume of sampled air (DTT_v, nmol min^{-1} m^{-3}) and the mass concentration of $PM_{2.5}$

192 (DTT_m, pmol min^{-1} $μg^{-1}$).

193 Considering that for samples containing a significant amount of substances

194 whose DTT response is non-linear with $PM_{2.5}$ concentration (e.g., Cu, Mn), the DTT_m

195 value depends on the concentration of $PM_{2.5}$ added to the reaction solution (Charrier

196 et al., 2016). The response of DTT_m to $PM_{2.5}$ concentration added to the reaction

197 solution was analyzed using sample containing high concentrations of soluble Cu and

198 Mn (Figure S2). When the $PM_{2.5}$ concentration added to the reaction solution is less

199 than 150 μg mL^{-1}, the DTT_m response is greatly affected by the difference in added

200 $PM_{2.5}$ concentration; however, when the $PM_{2.5}$ concentration added to the reaction

201 solution is greater than 150 μg mL^{-1}, the DTT_m response is less affected by the

202 difference in $PM_{2.5}$ concentration (< 12%). In this study, the concentration of $PM_{2.5}$

203   added to the reaction solution of most samples from the two sites was greater than 150

204     $\mu g \ mL^{-1}$ (ranged from 79 to 749 $\mu g \ mL^{-1}$, with an average of 409 ± 164 and 207 ± 95

205     $\mu g \ mL^{-1}$ in the south and north, respectively), therefore, the difference in $PM_{2.5}$

206   concentration added to the reaction solution of different samples should had a

207   relatively small impact on the difference in DTT_m values of different samples. This

208   study did not consider the impact of metal precipitation in phosphate matrix on the

209   measured DTT values, as there is not a straightforward method to correct the artifact

210   caused by this phenomenon (Yalamanchili et al., 2023).

211   **2.4 Source apportionment**

212   The sources of DTT activities were identified and quantified using PMF model

213   implemented by the multilinear engine (ME-2; (Paatero, 1997)) following the method

214   described in our previous studies (Huang et al., 2014; Yuan et al., 2020). For each site,

215   31 samples (a total of 62 samples) and 23 species were input into PMF model. The

216   number of samples is higher than the number of species. The input data include

217   species concentration (including DTT_v, 14 trace elements and 8 organic markers) and

218   uncertainties. The species-specific uncertainties were calculated following Liu et al.

219   (2017). For a clear separation of sources profiles, the contribution of corresponding

220   markers was set to 0 in the sources unrelated to the markers (see Table S1). More

221   details are described in SI (PMF analysis).

222

223   **3 Results and discussion**

224   **3.1 DTT activity and concentrations of water-soluble $PM_{2.5}$ components**

225   Figure 1 shows the daily variation of DTT activity, light absorption of WSOC at

226   wavelength 365 nm (Abs_{365}), together with the concentrations of $PM_{2.5}$, WSOC,

227   NACs and total elements in the south and north of Beijing. Their average values are

228   shown in Table S2. Generally, the average values of $PM_{2.5}$, WSOC, Abs_{365}, NACs and

229   total elements were higher in the south than in the north. Specifically, the

230   concentrations of $PM_{2.5}$ and WSOC in the south (122 ± 49 $\mu g \ m^{-3}$ and 8.1 ± 5.0 μgC

231   m^{-3}, respectively) were both about two times higher than that in the north (62 ± 28 μg

232 m^{-3} and 4.0 ± 2.0 μgC m^{-3}, respectively), indicating that the proportion of WSOC in

233 PM$_{2.5}$ was similar in the south and north. However, the Abs$_{365}$ in the south was about

234 three times that in the north, indicating that the chemical composition of WSOC was

235 different between the south and north. Previous studies have reported that NACs are

236 the main water-soluble light-absorbing organic compounds (also known as brown

237 carbon, BrC) of PM$_{2.5}$ (Lin et al., 2017; Huang et al., 2020; Li et al., 2020). For the 7

238 NACs quantified in this study, the total concentration of nitrophenols (4NP, 2M4NP

239 and 3M4NP), nitrocatechols (4NC, 3M5NC and 4M5NC), and 4N1N in the south

240 (108 ± 73 ng m^{-3}, 118 ± 91 ng m^{-3} and 12 ± 8.2 ng m^{-3}, respectively) was about three,

241 five and four times, respectively, those in the north (35 ± 22 ng m^{-3}, 24 ± 30 ng m^{-3}

242 and 3.1 ± 3.0 ng m^{-3}, respectively). These results indicate that the sources and

243 emission strength of water-soluble organic compounds were different in the south and

244 north of Beijing, suggesting the different contribution of water-soluble organic

245 compounds to DTT activity. The concentration trends of total trace elements were also

246 different between the south and north of Beijing, with Fe > Zn > Ti > Mn > Cu > Ba >

247 Pb > Sr > Cr > As > V > Ni > Cd > Co in the south, and Fe > Ti > Zn > Ba > Mn >

248 Pb > Cu > Cr > Sr > As > Ni > V > Cd > Co in the north. It should be noted that

249 although the contents of PM$_{2.5}$, WSOC and total elements measured in this study were

250 higher in the south than in the north, the average DTT$_v$ value in the south (3.9 ± 0.9

251 nmol min^{-1} m^{-3}) was comparable to that in the north (3.5 ± 1.2 nmol min^{-1} m^{-3}),

252 meanwhile, the average DTT$_m$ value was much higher (1.8 times) in the north (65 ±

253 28 pmol min^{-1} μg^{-1}) than in the south (36 ± 14 pmol min^{-1} μg^{-1}). Ahmad et al. (2021)

254 also reported that the concentrations of PM$_{2.5}$, WSOC, and most elements in Lahore,

255 Pakistan, were higher than those in Peshawar, Pakistan, while the DTT$_v$ values of the

256 two sites were similar, and the DTT$_m$ value in Peshawar was higher than that in

257 Lahore. The lower DTT$_m$ in the south than in the north may be due to the increased

258 PM$_{2.5}$ in the south containing more substances with no or little contribution to DTT

259 activity, and indicates that the intrinsic OP of water-soluble components of PM$_{2.5}$ was

260 higher in the north than in the south. The similar DTT$_v$ values in the south and north

indicate that the exposure-relevant OP of water-soluble components of $PM_{2.5}$ was comparable in the two sites, and the water-soluble DTT_v was not consistent with the content of water-soluble substances. Due to the complex chemical composition of $PM_{2.5}$, there may also be antagonistic and synergistic effects, contributing to the inconsistent relationship between DTT activity and compounds content (Xiong et al., 2017; Lionette et al., 2021).

Figure 2 shows the comparison of water-soluble $PM_{2.5}$ DTT activity measured in this study with those measured in other regions of Asia during similar periods. It can be seen that the DTT_v values measured in Beijing in this study were lower than that in Jinzhou, Tianjin, Yantai, and Shanghai in China, Lahore and Peshawar in Pakistan, and Delhi in India (Liu et al., 2018; Ahmad et al., 2021; Puthussery et al., 2022; Wu et al., 2022a), higher than that in Xi'an, Nanjing, Hangzhou, Guangzhou, and Shenzhen in China (Wang et al., 2019; Wang et al., 2020b; Ma et al., 2021; Yu et al., 2022c; Xing et al., 2023), and comparable with that in Ningbo, China (Chen et al., 2022). Different from DTT_v, the DTT_m value measured in NCNT in Beijing was similar with that in Jinzhou, Tianjin, Yantai, Shanghai and Ningbo in China (Liu et al., 2018; Chen et al., 2022; Wu et al., 2022a), and higher than that in other regions. The differences in water-soluble DTT activity of $PM_{2.5}$ in different regions can be explained by the differences in chemical composition, sources and atmospheric formation processes (Tong et al., 2017; Wong et al., 2019; Daellenbach et al., 2020; Wang et al., 2020b; Cao et al., 2021). For example, Cao et al. (2021) reported the water-soluble DTT activity of $PM_{2.5}$ from biomass and coal burning emissions in China, and the average value of biomass burning (4.5-7.4 pmol min^{-1} μg^{-1}) was much higher than that of coal burning (0.5-2.1 pmol min^{-1} μg^{-1}). Tuet et al. (2017) measured the water-soluble DTT activity of SOA generated under different precursors and reaction conditions, with SOA from naphthalene photooxidation under RO_2 + NO-dominant dry reaction conditions had the highest DTT activity.

3.2 Correlation between DTT activity and water-soluble $PM_{2.5}$ components

Figure 3 shows the correlations of DTT_v with $PM_{2.5}$, WSOC and Abs_{365} in the

290   south and north of Beijing. It can be seen that the correlation coefficient between

291   DTT_v and $PM_{2.5}$ was moderate in both the south (r = 0.42) and north (r = 0.45),

292   indicating that the OP of particles cannot be evaluated solely by the total $PM_{2.5}$

293   concentration. The correlations between DTT_v with WSOC and Abs_{365} were strong in

294   the north (r of 0.69 and 0.70, respectively), while relatively weak in the south (r of

295   0.41 and 0.40, respectively). The high correlations between DTT_v with WSOC and

296   Abs_{365} in the north of Beijing qualitatively agree with previous studies in Xi'an, China

297   and Atlanta, United States (Verma et al., 2012; Chen et al., 2019), and suggest that

298   water-soluble organic matter, especially BrC, has a significant contribution to DTT

299   consumption in the north. Light-absorbing BrC typically has conjugated electrons,

300   making it more likely to transport electrons for catalytic reactions, thereby

301   contributing to DTT activity (Chen et al., 2019; Wu et al., 2022). Further, in the north,

302   the DTT_v was closely related to the concentrations of NACs (r of 0.57 to 0.79) (Figure

303   S3), suggesting that NACs may be important contributors to DTT consumption. Feng

304   et al. (2022) reported the positive correlations between NACs and biomarkers in

305   saliva and urine (interleukin-6 and 8-hydrox-2′-deoxyguanosine). Zhang et al. (2023)

306   also reported that NACs are major proinflammatory components in organic aerosols,

307   contributing about 24% of the interleukin-8 response of all compounds detected by

308   Fourier transform ion cyclotron resonance mass spectrometry (FT-ICR-MS) in

309   electrospray ionization negative mode (ESI-). Certainly, it may also be other

310   substances related to NACs that contribute to the DTT activity, including those not

311   detected in this study, driving the good correlation between NACs and DTT_v in the

312   north of Beijing, which is worth studying in the future.

313   The correlation coefficients between DTT_v and 14 trace elements are shown in

314   Figure 4. Generally, the correlations between DTT_v and soluble elements were higher

315   than that between DTT_v and total elements in both the south and north of Beijing. For

316   soluble elements, in the south, the DTT_v showed positive correlations with Mn, Fe, Cr,

317   Co, As and Pb (r > 0.5), while in the north, it exhibited strong positive correlations

318   with Mn, Co, Ni, Zn, As, Cd and Pb (r > 0.7), indicating the different sources of DTT_v

319 in the south and north of Beijing. It is worth noting that the concentrations of all

320 soluble elements were higher in the south than in the north (Figure S4), while the

321 correlation between DTT_v and most soluble elements was lower in the south than in

322 the north (Figure 4). The high correlations between DTT_v and soluble elements in the

323 north of Beijing suggests that soluble elements also had a significant contribution to

324 DTT consumption. The low correlations between DTT_v and soluble elements in the

325 south of Beijing may be due to the nonlinear relationship between DTT consumption

326 and element concentration (Charrier and Anastasio, 2012; Wu et al., 2022a). As shown

327 in Figure S5, the relationship between most soluble trace elements and DTT_v was

328 more non-linear than linear. As the concentration of soluble elements increases, the

329 growth rate of DTT_v obviously decreases.

330 In addition to being associated with individual water-soluble species, the

331 interactions between metals and organic compounds also affect the consumption of

332 DTT (Xiong et al., 2017; Wu et al., 2022b), with both synergistic and antagonistic

333 effects. For example, Wu et al. (2022b) measured the DTT consumption of Fe(III) and

334 Cu(II) interacting with 1,4-naphthoquinone, 9,10-phenanthraquinone, citric acid, and

335 4-nitrocatechol, respectively. Their results showed that Cu(II) had antagonistic effects

336 in interacting with most organics except for citric acid, and Fe(III) had an additive

337 effect on DTT consumption of 1,4-naphthoquinone and citric acid, while it had an

338 antagonistic effect on 1,4-naphthoquinone and 9,10-phenanthraquinone. Due to the

339 complex composition of water-soluble organic aerosols, the knowledge about the

340 effects of organics and metal-organic interactions on DTT activity are still limited,

341 especially the effects of BrC chromophores and their interactions with metals.

342 **3.3 Sources of DTT activity**

343 This study analyzed eight organic markers (including levoglucosan, mannosan,

344 and galactosan for biomass burning, hopanes for vehicle emissions, picene for coal

345 combustion, and phthalic acid, isophthalic acid and terephthalic acid for secondary

346 formation) to help identify the sources of DTT activity. The average concentrations of

347 these organic markers are shown in Table S2. The correlation coefficients between

348 DTT$_v$ and organic markers are shown in Figure S6. In the south, levoglucosan,

349 mannosan, galactosan, and hopanes had moderate correlation with DTT$_v$ (r of 0.41 to

350 0.48); phthalic acid, isophthalic acid and terephthalic acid had low to moderate

351 correlation with DTT$_v$ (r of 0.28 to 0.54); picene had low correlation with DTT$_v$ (r of

352 0.21). These results suggest that biomass burning and vehicle emissions could have

353 significant contribution to water-soluble PM$_{2.5}$ OP in the south. In the north, hopanes

354 had the highest correlation with DTT$_v$ (r = 0.70), indicating that vehicle emissions

355 could have an important contribution. Levoglucosan, mannosan, galactosan, phthalic

356 acid, isophthalic acid, terephthalic acid, and picene had moderate to high correlations

357 with DTT$_v$ in the north, suggesting that biomass and coal burning, and secondary

358 formation may also have certain contribution to water-soluble PM$_{2.5}$ OP.

359   To further quantify the sources of DTT activity in the south and the north of

360 Beijing, the PMF model, which was widely used for the source apportionment of

361 PM$_{2.5}$ OP (Liu et al., 2018; Shen et al., 2022; Cui et al., 2023), was applied. The input

362 species include DTT$_v$, soluble elements and organic markers, and five to seven factors

363 were examined. Due to the oil factor mixed with vehicle emissions factor in the five-

364 factor solution, and there was no new reasonable factor when increasing the factor

365 number to seven in the PMF analysis (Figure S7). Finally, six factors were resolved

366 and quantified using PMF model in the south and north of Beijing, including biomass

367 burning, coal burning, traffic-related, dust, oil combustion, and secondary formation,

368 and the profiles of these sources are shown in Figure S8. The uncertainties of PMF

369 analysis for these sources were 2-14%. Factor 1 is characterized by high contribution

370 of levoglucosan, mannosan, and galactosan, mainly from biomass burning (Huang et

371 al., 2014; Chow et al., 2022). The DTT activity of biomass burning organic aerosol

372 was measured by Wong et al. (2019), which was 48 ± 6 pmol min^{-1} μg^{-1} of WSOC.

373 Liu et al. (2018) quantified the sources of DTT$_v$ in coastal cities (Jinzhou, Tianjin, and

374 Yantai) in China with PMF model and multiple linear regression method, and the

375 results showed that biomass burning contributed 28% on average in winter. Factor 2

376 exhibits a large fraction of picene, Zn, Mn, Cd, As, and Pb, which is considered to be

13

coal burning (Huang et al., 2014; Huang et al., 2018). Joo et al. (2018) measured the DTT activity of $PM_{2.5}$ emitted from coal combustion at different temperatures, with the highest values of 26 ± 21 pmol min^{-1} μg^{-1} and 0.10 ± 0.06 nmol min^{-1} m^{-3} occurring at 550 °C. Factor 3 is identified as traffic-related emissions, which is characterized by the higher loading of hopanes, Ba, Sr, Cu and Ni (Huang et al., 2018; Chow et al., 2022). Vreeland et al. (2017) measured the DTT activity of $PM_{2.5}$ emitted by side street and highway vehicles in Atlanta, with values of 0.78 ± 0.60 nmol min^{-1} m^{-3} and 1.1 ± 0.60 nmol min^{-1} m^{-3}, respectively. Ting et al. (2023) reported that the DTT activity of $PM_{2.5}$ from vehicle emissions in Ziqing tunnel in Taiwan, China, was 0.15-0.46 nmol min^{-1} m^{-3}. Factor 4, secondary formation, which is identified by high levels of phthalic acid, isophthalic acid, and terephthalic acid (Al-Naiema and Stone, 2017; Wang et al., 2020a). Verma et al. (2014) reported that secondary formation contributed about 30% to the water-soluble DTT activity of $PM_{2.5}$ in urban Atlanta. It is worth noting that the DTT activity of SOA generated from different precursors is different (Tuet et al., 2017; Tong et al., 2018). For example, the DTT activity of SOA from naphthalene was higher than that from isoprene (Tuet et al., 2017; Tong et al., 2018). Factor 5 is dominated by crustal elements Fe and Ti, mainly from dust (Huang et al., 2018). The DTT activity of atmospheric particulate matter during dust periods were reported in previous studies (Chirizzi et al., 2017; Khoshnamvand et al., 2023) and it has a low contribution in this study. Factor 6 is identified as oil combustion because of the high levels of V and Ni (Moreno et al., 2011; Minguillón et al., 2014; Huang et al., 2018).

The source contributions of DTT_v in the south and north of Beijing are shown in Figure 5, exhibiting obvious district differences. In the south, traffic-related emissions (39%) and biomass burning (25%) had the most contribution to DTT_v, followed by secondary formation (17%), coal burning (15%), dust (2%), and oil combustion (2%). In the north, traffic-related emissions (52%) had the highest contribution to DTT_v, followed by coal burning (20%), secondary formation (13%), biomass burning (8%), oil combustion (4%), and dust (3%). The absolute contribution of each source to

406   DTT_v varies by 1.2-3.4 times between the south and north of Beijing (Table S3). The

407   large district differences in sources of DTT_v of water-soluble $PM_{2.5}$ call for more

408   research on the relationship between sources, chemical composition, formation

409   processes and OP of $PM_{2.5}$.

410

411   **4 Conclusions**

412   In this study, the water-soluble OP of ambient $PM_{2.5}$ collected in winter in the

413   south and north of Beijing were quantified, together with the concentration and light

414   absorption of WSOC, and concentrations of 7 light-absorbing NACs and 14 trace

415   elements. The average DTT_v value was comparable in the south (3.9 ± 0.9 nmol min^{-1}

416   m^{-3}) and north (3.5 ± 1.2 nmol min^{-1} m^{-3}), while the DTT_m was higher in the north (65

417   ± 28 pmol min^{-1} µg^{-1}) than in the south (36 ± 14 pmol min^{-1} µg^{-1}), indicating that the

418   exposure-relevant OP of water-soluble components of $PM_{2.5}$ was similar in the two

419   sites and that the intrinsic OP of water-soluble components of $PM_{2.5}$ was higher in the

420   north than in the south. The correlation between DTT_v and soluble elements was

421   higher than that between DTT_v and total elements in both the south and north. In the

422   north, the DTT_v was strongly correlated with soluble Mn, Co, Ni, Zn, As, Cd and Pb

423   ($r > 0.7$), and in the south it positively correlated with Mn, Fe, Cr, Co, As and Pb ($r >$

424   0.5). In addition, in the north the DTT_v was also positively correlated with WSOC,

425   Abs_{365} and NACs (r of 0.56 to 0.79), while in the south it was weakly correlated ($r \leq$

426   0.4). These results indicate that in the north trace elements and water-soluble organic

427   compounds, especially BrC chromophores, both had significant contributions to DTT

428   consumption, and in the south the consumption of DTT may be mainly from trace

429   elements. Six sources of DTT_v were resolved with the PMF model, including biomass

430   burning, coal burning, traffic-related, dust, oil combustion, and secondary formation.

431   On average, traffic-related emissions (39%) and biomass burning (25%) were the

432   major contributors of DTT_v in the south, and traffic-related emissions (52%) was the

433   predominated source in the north. The differences in DTT_v sources in the south and

434   north of Beijing suggest that the relationship between source emissions and

15

atmospheric processes and $PM_{2.5}$ OP deserve further exploration in order to better understand the regional differences of health impacts of $PM_{2.5}$. Besides, in order to gain a more comprehensive understanding of the regional differences in $PM_{2.5}$ OP, sources and its relationship with chemical composition, longer periods and different seasonal datasets are also need to be studied in the future.

Date availability. Raw data used in this study can be obtained from the following open link: https://doi.org/10.5281/zenodo.10791126 (Yuan et al., 2024). It is also available on request by contacting the corresponding author.

Supplement. The Supplement related to this article is available online.

Author contributions. RJH designed the study. Data analysis was done by WY, CL, LY, HY and RJH. WY, CL, LY, HY and RJH interpreted data, prepared the display items and wrote the manuscript. All authors commented on and discussed the manuscript.

Competing interests. The authors declare that they have no conflict of interest.

References

Ahmad, M., Yu, Q., Chen, J., Cheng, S., Qin, W., and Zhang, Y.: Chemical characteristics, oxidative potential, and sources of PM$_{2.5}$ in wintertime in Lahore and Peshawar, Pakistan, J. Environ. Sci., 102, 148-158, 10.1016/j.jes.2020.09.014, 2021.

Al-Naiema, I. M. and Stone, E. A.: Evaluation of anthropogenic secondary organic aerosol tracers from aromatic hydrocarbons, Atmos. Chem. Phys., 17, 2053-2065, 10.5194/acp-17-2053-2017, 2017.

An, Z., Huang, R. J., Zhang, R., Tie, X., Li, G., Cao, J., Zhou, W., Shi, Z., Han, Y., Gu, Z., and Ji, Y.: Severe haze in northern China: A synergy of anthropogenic emissions and atmospheric processes, Proc. Natl. Acad. Sci. U. S. A., 116, 8657-8666, 10.1073/pnas.1900125116, 2019.

Bates, J. T., Fang, T., Verma, V., Zeng, L., Weber, R. J., Tolbert, P. E., Abrams, J. Y., Sarnat, S. E., Klein, M., Mulholland, J. A., and Russell, A. G.: Review of Acellular Assays of Ambient Particulate Matter Oxidative Potential: Methods and Relationships with Composition, Sources, and Health Effects, Environ. Sci. Technol., 53, 4003-4019, 10.1021/acs.est.8b03430, 2019.

Besis, A., Romano, M. P., Serafeim, E., Avgenikou, A., Kouras, A., Lionetto, M. G., Guascito, M. R., De Bartolomeo, A. R., Giordano, M. E., Mangone, A., Contini, D., and Samara, C.: Size-Resolved Redox Activity and Cytotoxicity of Water-Soluble Urban Atmospheric Particulate Matter: Assessing

Contributions from Chemical Components, Toxics, 11, 10.3390/toxics11010059, 2023.

Burnett, R., Chen, H., Szyszkowicz, M., Fann, N., Hubbell, B., Pope, C. A., 3rd, Apte, J. S., Brauer, M., Cohen, A., Weichenthal, S., Coggins, J., Di, Q., Brunekreef, B., Frostad, J., Lim, S. S., Kan, H., Walker, K. D., Thurston, G. D., Hayes, R. B., Lim, C. C., Turner, M. C., Jerrett, M., Krewski, D., Gapstur, S. M., Diver, W. R., Ostro, B., Goldberg, D., Crouse, D. L., Martin, R. V., Peters, P., Pinault, L., Tjepkema, M., van Donkelaar, A., Villeneuve, P. J., Miller, A. B., Yin, P., Zhou, M., Wang, L., Janssen, N. A. H., Marra, M., Atkinson, R. W., Tsang, H., Quoc Thach, T., Cannon, J. B., Allen, R. T., Hart, J. E., Laden, F., Cesaroni, G., Forastiere, F., Weinmayr, G., Jaensch, A., Nagel, G., Concin, H., and Spadaro, J. V.: Global estimates of mortality associated with long-term exposure to outdoor fine particulate matter, Proc. Natl. Acad. Sci. U. S. A., 115, 9592-9597, 10.1073/pnas.1803222115, 2018.

Calas, A., Uzu, G., Kelly, F. J., Houdier, S., Martins, J. M. F., Thomas, F., Molton, F., Charron, A., Dunster, C., Oliete, A., Jacob, V., Besombes, J.-L., Chevrier, F., and Jaffrezo, J.-L.: Comparison between five acellular oxidative potential measurement assays performed with detailed chemistry on PM_{10} samples from the city of Chamonix (France), Atmos. Chem. Phys., 18, 7863-7875, 10.5194/acp-18-7863-2018, 2018.

Campbell, S. J., Wolfer, K., Utinger, B., Westwood, J., Zhang, Z. H., Bukowiecki, N., Steimer, S. S., Vu, T. V., Xu, J., Straw, N., Thomson, S., Elzein, A., Sun, Y., Liu, D., Li, L., Fu, P., Lewis, A. C., Harrison, R. M., Bloss, W. J., Loh, M., Miller, M. R., Shi, Z., and Kalberer, M.: Atmospheric conditions and composition that influence $PM_{2.5}$ oxidative potential in Beijing, China, Atmos. Chem. Phys., 21, 5549-5573, 10.5194/acp-21-5549-2021, 2021.

Cao, T., Li, M., Zou, C., Fan, X., Song, J., Jia, W., Yu, C., Yu, Z., and Peng, P. a.: Chemical composition, optical properties, and oxidative potential of water- and methanol-soluble organic compounds emitted from the combustion of

biomass materials and coal, Atmos. Chem. Phys., 21, 13187-13205, 10.5194/acp-21-13187-2021, 2021.

Charrier, J. G. and Anastasio, C.: On dithiothreitol (DTT) as a measure of oxidative potential for ambient particles: evidence for the importance of soluble transition metals, Atmos. Chem. Phys., 12, 9321-9333, 10.5194/acp-12-9321-2012, 2012.

Charrier, J. G., McFall, A. S., Vu, K. K.-T., Baroi, J., Olea, C., Hasson, A., and Anastasio, C.: A Bias in the "Mass-Normalized" DTT Response-An Effect of Non-Linear Concentration Response Curves for Copper and Manganese, Atmos. Environ., 144, 325-334, 2016.

Chen, K., Xu, J., Famiyeh, L., Sun, Y., Ji, D., Xu, H., Wang, C., Metcalfe, S. E., Betha, R., Behera, S. N., Jia, C., Xiao, H., and He, J.: Chemical constituents, driving factors, and source apportionment of oxidative potential of ambient fine particulate matter in a Port City in East China, J. Hazard. Mater., 440, 10.1016/j.jhazmat.2022.129864, 2022.

Chen, Q., Wang, M., Wang, Y., Zhang, L., Li, Y., and Han, Y.: Oxidative Potential of Water-Soluble Matter Associated with Chromophoric Substances in $PM_{2.5}$ over Xi'an, China, Environ. Sci. Technol., 53, 8574-8584, 10.1021/acs.est.9b01976, 2019.

Chirizzi, D., Cesari, D., Guascito, M. R., Dinoi, A., Giotta, L., Donateo, A., and Contini, D.: Influence of Saharan dust outbreaks and carbon content on oxidative potential of water-soluble fractions of $PM_{2.5}$ and PM_{10}, Atmos. Environ., 163, 1-8, 10.1016/j.atmosenv.2017.05.021, 2017.

Chow, W. S., Huang, X. H. H., Leung, K. F., Huang, L., Wu, X., and Yu, J. Z.: Molecular and elemental marker-based source apportionment of fine particulate matter at six sites in Hong Kong, China, Sci. Total Environ., 813, 152652, 10.1016/j.scitotenv.2021.152652, 2022.

Chowdhury, P. H., He, Q., Carmieli, R., Li, C., Rudich, Y., and Pardo, M.: Connecting the Oxidative Potential of Secondary Organic Aerosols with Reactive Oxygen

Species in Exposed Lung Cells, Environ. Sci. Technol., 53, 13949-13958, 10.1021/acs.est.9b04449, 2019.

Cui, Y., Zhu, L., Wang, H., Zhao, Z., Ma, S., and Ye, Z.: Characteristics and Oxidative Potential of Ambient $PM_{2.5}$ in the Yangtze River Delta Region: Pollution Level and Source Apportionment, Atmosphere, 14, 10.3390/atmos14030425, 2023.

Daellenbach, K. R., Uzu, G., Jiang, J., Cassagnes, L. E., Leni, Z., Vlachou, A., Stefenelli, G., Canonaco, F., Weber, S., Segers, A., Kuenen, J. J. P., Schaap, M., Favez, O., Albinet, A., Aksoyoglu, S., Dommen, J., Baltensperger, U., Geiser, M., El Haddad, I., Jaffrezo, J. L., and Prevot, A. S. H.: Sources of particulate-matter air pollution and its oxidative potential in Europe, Nature, 587, 414-419, 10.1038/s41586-020-2902-8, 2020.

Fan, X., Li, M., Cao, T., Cheng, C., Li, F., Xie, Y., Wei, S., Song, J., and Peng, P. a.: Optical properties and oxidative potential of water- and alkaline-soluble brown carbon in smoke particles emitted from laboratory simulated biomass burning, Atmos. Environ., 194, 48-57, 10.1016/j.atmosenv.2018.09.025, 2018.

Fang, T., Verma, V., Bates, J. T., Abrams, J., Klein, M., Strickland, M. J., Sarnat, S. E., Chang, H. H., Mulholland, J. A., Tolbert, P. E., Russell, A. G., and Weber, R. J.: Oxidative potential of ambient water-soluble $PM_{2.5}$ in the southeastern United States: contrasts in sources and health associations between ascorbic acid (AA) and dithiothreitol (DTT) assays, Atmos. Chem. Phys., 16, 3865-3879, 10.5194/acp-16-3865-2016, 2016.

Feng, R., Xu, H., Gu, Y., Wang, Z., Han, B., Sun, J., Liu, S., Lu, H., Ho, S. S. H., Shen, Z., and Cao, J.: Variations of Personal Exposure to Particulate Nitrated Phenols from Heating Energy Renovation in China: The First Assessment on Associated Toxicological Impacts with Particle Size Distributions, Environ. Sci. Technol., 56, 3974−3983, 2022.

Gao, D., Fang, T., Verma, V., Zeng, L., and Weber, R. J.: A method for measuring total aerosol oxidative potential (OP) with the dithiothreitol (DTT) assay and comparisons between an urban and roadside site of water-soluble and total OP,

580   Atmos. Meas. Tech., 10, 2821-2835, 10.5194/amt-10-2821-2017, 2017.

581 Guascito, M. R., Lionetto, M. G., Mazzotta, F., Conte, M., Giordano, M. E., Caricato,

582   R., De Bartolomeo, A. R., Dinoi, A., Cesari, D., Merico, E., Mazzotta, L., and

583   Contini, D.: Characterisation of the correlations between oxidative potential

584   and in vitro biological effects of PM_{10} at three sites in the central

585   Mediterranean, J. Hazard. Mater., 448, 130872,

586   10.1016/j.jhazmat.2023.130872, 2023.

587 Hecobian, A., Zhang, X., Zheng, M., Frank, N., Edgerton, E. S., and Weber, R. J.:

588   Water-Soluble Organic Aerosol material and the light-absorption

589   characteristics of aqueous extracts measured over the Southeastern United

590   States, Atmos. Chem. Phys., 10, 5965-5977, 10.5194/acp-10-5965-2010, 2010.

591 Ho, K. F., Ho, S. S. H., Huang, R.-J., Liu, S. X., Cao, J.-J., Zhang, T., Chuang, H.-C.,

592   Chan, C. S., Hu, D., and Tian, L.: Characteristics of water-soluble organic

593   nitrogen in fine particulate matter in the continental area of China, Atmos.

594   Environ., 106, 252-261, 10.1016/j.atmosenv.2015.02.010, 2015.

595 Huang, R. J., Cheng, R., Jing, M., Yang, L., Li, Y., Chen, Q., Chen, Y., Yan, J., Lin, C.,

596   Wu, Y., Zhang, R., El Haddad, I., Prevot, A. S. H., O'Dowd, C. D., and Cao, J.:

597   Source-Specific Health Risk Analysis on Particulate Trace Elements: Coal

598   Combustion and Traffic Emission As Major Contributors in Wintertime

599   Beijing, Environ. Sci. Technol., 52, 10967-10974, 10.1021/acs.est.8b02091,

600   2018.

601 Huang, R. J., Yang, L., Shen, J., Yuan, W., Gong, Y., Guo, J., Cao, W., Duan, J., Ni, H.,

602   Zhu, C., Dai, W., Li, Y., Chen, Y., Chen, Q., Wu, Y., Zhang, R., Dusek, U.,

603   O'Dowd, C., and Hoffmann, T.: Water-Insoluble Organics Dominate Brown

604   Carbon in Wintertime Urban Aerosol of China: Chemical Characteristics and

605   Optical Properties, Environ. Sci. Technol., 54, 7836-7847,

606   10.1021/acs.est.0c01149, 2020.

607 Huang, R. J., Zhang, Y., Bozzetti, C., Ho, K. F., Cao, J. J., Han, Y., Daellenbach, K. R.,

608   Slowik, J. G., Platt, S. M., Canonaco, F., Zotter, P., Wolf, R., Pieber, S. M.,

Bruns, E. A., Crippa, M., Ciarelli, G., Piazzalunga, A., Schwikowski, M., Abbaszade, G., Schnelle-Kreis, J., Zimmermann, R., An, Z., Szidat, S., Baltensperger, U., El Haddad, I., and Prevot, A. S.: High secondary aerosol contribution to particulate pollution during haze events in China, Nature, 514, 218-222, 10.1038/nature13774, 2014.

Jiang, H., Xie, Y., Ge, Y., He, H., and Liu, Y.: Effects of ultrasonic treatment on dithiothreitol (DTT) assay measurements for carbon materials, J. Environ. Sci., 84, 51–58, 2019.

Joo, H. S., Batmunkh, T., Borlaza, L. J. S., Park, M., Lee, K. Y., Lee, J. Y., Chang, Y. W., and Park, K.: Physicochemical properties and oxidative potential of fine particles produced from coal combustion, Aerosol Sci. Technol., 52, 1134-1144, 10.1080/02786826.2018.1501152, 2018.

Khoshnamvand, N., Nodehi, R. N., Hassanvand, M. S., and Naddafi, K.: Comparison between oxidative potentials measured of water-soluble components in ambient air PM_1 and $PM_{2.5}$ of Tehran, Iran, Air Qual. Atmos. Hlth., 16, 1311-1320, 10.1007/s11869-023-01343-y, 2023.

Laskin, A., Laskin, J., and Nizkorodov, S. A.: Chemistry of atmospheric brown carbon, Chem. Rev., 115, 4335-4382, 10.1021/cr5006167, 2015.

Lelieveld, S., Wilson, J., Dovrou, E., Mishra, A., Lakey, P. S. J., Shiraiwa, M., Poschl, U., and Berkemeier, T.: Hydroxyl Radical Production by Air Pollutants in Epithelial Lining Fluid Governed by Interconversion and Scavenging of Reactive Oxygen Species, Environ. Sci. Technol., 55, 14069-14079, 10.1021/acs.est.1c03875, 2021.

Lin, P., Bluvshtein, N., Rudich, Y., Nizkorodov, S. A., Laskin, J., and Laskin, A.: Molecular chemistry of atmospheric brown carbon inferred from a nationwide biomass burning event, Environ. Sci. Technol., 51, 11561–11570, 2017.

Lionetto, M., Guascito, M., Giordano, M., Caricato, R., De Bartolomeo, A., Romano, M., Conte, M., Dinoi, A., and Contini, D.: Oxidative Potential, Cytotoxicity, and Intracellular Oxidative Stress Generating Capacity of PM_{10}: A Case Study

in South of Italy, Atmosphere, 12, 10.3390/atmos12040464, 2021.

Liu, W., Xu, Y., Liu, W., Liu, Q., Yu, S., Liu, Y., Wang, X., and Tao, S.: Oxidative potential of ambient $PM_{2.5}$ in the coastal cities of the Bohai Sea, northern China: Seasonal variation and source apportionment, Environ. Pollut., 236, 514-528, 10.1016/j.envpol.2018.01.116, 2018.

Liu, Y., Yan, C. Q., Ding, X., Wang, X. M., Fu, Q. Y., Zhao, Q. B., Zhang, Y. H., Duan, Y. S., Qiu, X. H., and Zheng, M.: Sources and spatial distribution of particulate polycyclic aromatic hydrocarbons in Shanghai, China, Sci. Total Environ., 584-585, 307-317, https://doi.org/10.1016/j.scitotenv.2016.12.134, 2017.

Ma, X., Nie, D., Chen, M., Ge, P., Liu, Z., Ge, X., Li, Z., and Gu, R.: The Relative Contributions of Different Chemical Components to the Oxidative Potential of Ambient Fine Particles in Nanjing Area, Int. J. Environ. Res. Public Health, 18, 2789, 10.3390/ijerph18062789, 2021.

Miljevic, B., Hedayat, F., Stevanovic, S., Fairfull-Smith, K. E., Bottle, S. E., and Ristovski, Z. D.: To sonicate or not to sonicate PM filters: reactive oxygen species generation upon ultrasonic irradiation, Aerosol. Sci. Technol., 48, 1276-1284, 2014.

Minguillón, M. C., Cirach, M., Hoek, G., Brunekreef, B., Tsai, M., de Hoogh, K., Jedynska, A., Kooter, I. M., Nieuwenhuijsen, M., and Querol, X.: Spatial variability of trace elements and sources for improved exposure assessment in Barcelona, Atmos. Environ., 89, 268-281, 10.1016/j.atmosenv.2014.02.047, 2014.

Moreno, T., Querol, X., Alastuey, A., Reche, C., Cusack, M., Amato, F., Pandolfi, M., Pey, J., Richard, A., Prévôt, A. S. H., Furger, M., and Gibbons, W.: Variations in time and space of trace metal aerosol concentrations in urban areas and their surroundings, Atmos. Chem. Phys., 11, 9415-9430, 10.5194/acp-11-9415-2011, 2011.

Oh, S. H., Park, K., Park, M., Song, M., Jang, K. S., Schauer, J. J., Bae, G. N., and

667   Bae, M. S.: Comparison of the sources and oxidative potential of $PM_{2.5}$ during
668   winter time in large cities in China and South Korea, Sci. Total Environ., 859,
669   160369, 10.1016/j.scitotenv.2022.160369, 2023.

670 Paatero, P.: Least squares formation of robust non negative factor analysis,
671   Chemometr. Intell. Lab., 37, 23-35, 1997.

672 Puthussery, J. V., Dave, J., Shukla, A., Gaddamidi, S., Singh, A., Vats, P., Salana, S.,
673   Ganguly, D., Rastogi, N., Tripathi, S. N., and Verma, V.: Effect of Biomass
674   Burning, Diwali Fireworks, and Polluted Fog Events on the Oxidative
675   Potential of Fine Ambient Particulate Matter in Delhi, India, Environ. Sci.
676   Technol., 56, 14605-14616, 10.1021/acs.est.2c02730, 2022.

677 Saffari, A., Daher, N., Shafer, M. M., Schauer, J. J., and Sioutas, C.: Global
678   perspective on the oxidative potential of airborne particulate matter: a
679   synthesis of research findings, Environ. Sci. Technol., 48, 7576-7583,
680   10.1021/es500937x, 2014.

681 Shafer, M. M., Hemming, J. D., Antkiewicz, D. S., and Schauer, J. J.: Oxidative
682   potential of size-fractionated atmospheric aerosol in urban and rural sites
683   across Europe, Faraday Discuss., 189, 381-405, 10.1039/c5fd00196j, 2016.

684 Shen, J., Taghvaee, S., La, C., Oroumiyeh, F., Liu, J., Jerrett, M., Weichenthal, S., Del
685   Rosario, I., Shafer, M. M., Ritz, B., Zhu, Y., and Paulson, S. E.: Aerosol
686   Oxidative Potential in the Greater Los Angeles Area: Source Apportionment
687   and Associations with Socioeconomic Position, Environ. Sci. Technol., 56,
688   17795-17804, 10.1021/acs.est.2c02788, 2022.

689 Ting, Y. C., Chang, P. K., Hung, P. C., Chou, C. C., Chi, K. H., and Hsiao, T. C.:
690   Characterizing emission factors and oxidative potential of motorcycle
691   emissions in a real-world tunnel environment, Environ. Res., 234, 116601,
692   10.1016/j.envres.2023.116601, 2023.

693 Tong, H., Lakey, P. S. J., Arangio, A. M., Socorro, J., Kampf, C. J., Berkemeier, T.,
694   Brune, W. H., Poschl, U., and Shiraiwa, M.: Reactive oxygen species formed
695   in aqueous mixtures of secondary organic aerosols and mineral dust

696   influencing cloud chemistry and public health in the Anthropocene, Faraday

697   Discuss., 200, 251-270, 10.1039/c7fd00023e, 2017.

698 Tong, H., Lakey, P. S. J., Arangio, A. M., Socorro, J., Shen, F., Lucas, K., Brune, W.

699   H., Poschl, U., and Shiraiwa, M.: Reactive Oxygen Species Formed by

700   Secondary Organic Aerosols in Water and Surrogate Lung Fluid, Environ. Sci.

701   Technol., 52, 11642-11651, 10.1021/acs.est.8b03695, 2018.

702 Tuet, W. Y., Chen, Y., Xu, L., Fok, S., Gao, D., Weber, R. J., and Ng, N. L.: Chemical

703   oxidative potential of secondary organic aerosol (SOA) generated from the

704   photooxidation of biogenic and anthropogenic volatile organic compounds,

705   Atmos. Chem. Phys., 17, 839-853, 10.5194/acp-17-839-2017, 2017.

706 Tuet, W. Y., Liu, F., de Oliveira Alves, N., Fok, S., Artaxo, P., Vasconcellos, P.,

707   Champion, J. A., and Ng, N. L.: Chemical Oxidative Potential and Cellular

708   Oxidative Stress from Open Biomass Burning Aerosol, Environ. Sci. Technol.

709   Lett., 6, 126-132, 10.1021/acs.estlett.9b00060, 2019.

710 Verma, V., Fang, T., Xu, L., Peltier, R. E., Russell, A. G., Ng, N. L., and Weber, R. J.:

711   Organic aerosols associated with the generation of reactive oxygen species

712   (ROS) by water-soluble $PM_{2.5}$, Environ. Sci. Technol., 49, 4646-4656,

713   10.1021/es505577w, 2015.

714 Verma, V., Rico-Martinez, R., Kotra, N., King, L., Liu, J., Snell, T. W., and Weber, R.

715   J.: Contribution of water-soluble and insoluble components and their

716   hydrophobic/hydrophilic subfractions to the reactive oxygen species-

717   generating potential of fine ambient aerosols, Environ. Sci. Technol., 46,

718   11384-11392, 10.1021/es302484r, 2012.

719 Verma, V., Fang, T., Guo, H., King, L., Bates, J. T., Peltier, R. E., Edgerton, E.,

720   Russell, A. G., and Weber, R. J.: Reactive oxygen species associated with

721   water-soluble $PM_{2.5}$ in the southeastern United States: spatiotemporal trends

722   and source apportionment, Atmos. Chem. Phys., 14, 12915-12930,

723   10.5194/acp-14-12915-2014, 2014.

724 Vreeland, H., Weber, R., Bergin, M., Greenwald, R., Golan, R., Russell, A. G., Verma,

V., and Sarnat, J. A.: Oxidative potential of $PM_{2.5}$ during Atlanta rush hour: Measurements of in-vehicle dithiothreitol (DTT) activity, Atmos. Environ., 165, 169-178, 10.1016/j.atmosenv.2017.06.044, 2017.

Wang, J., Lin, X., Lu, L., Wu, Y., Zhang, H., Lv, Q., Liu, W., Zhang, Y., and Zhuang, S.: Temporal variation of oxidative potential of water soluble components of ambient $PM_{2.5}$ measured by dithiothreitol (DTT) assay, Sci. Total Environ., 649, 969-978, 10.1016/j.scitotenv.2018.08.375, 2019.

Wang, T., Huang, R. J., Li, Y., Chen, Q., Chen, Y., Yang, L., Guo, J., Ni, H., Hoffmann, T., Wang, X., and Mai, B.: One-year characterization of organic aerosol markers in urban Beijing: Seasonal variation and spatiotemporal comparison, Sci. Total Environ., 743, 140689, 10.1016/j.scitotenv.2020.140689, 2020a.

Wang, Y., Wang, M., Li, S., Sun, H., Mu, Z., Zhang, L., Li, Y., and Chen, Q.: Study on the oxidation potential of the water-soluble components of ambient $PM_{2.5}$ over Xi'an, China: Pollution levels, source apportionment and transport pathways, Environ. Int., 136, 105515, 10.1016/j.envint.2020.105515, 2020b.

Wong, J. P. S., Tsagkaraki, M., Tsiodra, I., Mihalopoulos, N., Violaki, K., Kanakidou, M., Sciare, J., Nenes, A., and Weber, R. J.: Effects of Atmospheric Processing on the Oxidative Potential of Biomass Burning Organic Aerosols, Environ. Sci. Technol., 53, 6747-6756, 10.1021/acs.est.9b01034, 2019.

Wu, N., Lu, B., Chen, Q., Chen, J., and Li, X.: Connecting the Oxidative Potential of Fractionated Particulate Matter With Chromophoric Substances, J. Geophys. Res-Atmos., 127, 10.1029/2021jd035503, 2022a.

Wu, N., Lyu, Y., Lu, B., Cai, D., Meng, X., and Li, X.: Oxidative potential induced by metal-organic interaction from $PM_{2.5}$ in simulated biological fluids, Sci. Total Environ., 848, 157768, 10.1016/j.scitotenv.2022.157768, 2022b.

Xing, C., Wang, Y., Yang, X., Zeng, Y., Zhai, J., Cai, B., Zhang, A., Fu, T. M., Zhu, L., Li, Y., Wang, X., and Zhang, Y.: Seasonal variation of driving factors of ambient $PM_{2.5}$ oxidative potential in Shenzhen, China, Sci. Total Environ., 862, 160771, 10.1016/j.scitotenv.2022.160771, 2023.

Xiong, Q., Yu, H., Wang, R., Wei, J., and Verma, V.: Rethinking Dithiothreitol-Based Particulate Matter Oxidative Potential: Measuring Dithiothreitol Consumption versus Reactive Oxygen Species Generation, Environ. Sci. Technol., 51, 6507-6514, 10.1021/acs.est.7b01272, 2017.

Yalamanchili, J., Hennigan, C. J., and Reed, B. E.: Measurement artifacts in the dithiothreitol (DTT) oxidative potential assay caused by interactions between aqueous metals and phosphate buffer, J. Hazard. Mater., 456, 131693, 2023.

Yu, H., Wei, J., Cheng, Y., Subedi, K., and Verma, V.: Synergistic and Antagonistic Interactions among the Particulate Matter Components in Generating Reactive Oxygen Species Based on the Dithiothreitol Assay, Environ. Sci. Technol., 52, 2261–2270, 2018.

Yu, Q., Chen, J., Qin, W., Ahmad, M., Zhang, Y., Sun, Y., Xin, K., and Ai, J.: Oxidative potential associated with water-soluble components of $PM_{2.5}$ in Beijing: The important role of anthropogenic organic aerosols, J. Hazard. Mater., 433, 128839, 10.1016/j.jhazmat.2022.128839, 2022a.

Yu, S., Liu, W., Xu, Y., Yi, K., Zhou, M., Tao, S., and Liu, W.: Characteristics and oxidative potential of atmospheric $PM_{2.5}$ in Beijing: Source apportionment and seasonal variation, Sci. Total Environ., 650, 277-287, 10.1016/j.scitotenv.2018.09.021, 2019.

Yu, Y., Sun, Q., Li, T., Ren, X., Lin, L., Sun, M., Duan, J., and Sun, Z.: Adverse outcome pathway of fine particulate matter leading to increased cardiovascular morbidity and mortality: An integrated perspective from toxicology and epidemiology, J. Hazard. Mater., 430, 128368, 10.1016/j.jhazmat.2022.128368, 2022b.

Yu, Y., Cheng, P., Li, Y., Gu, J., Gong, Y., Han, B., Yang, W., Sun, J., Wu, C., Song, W., and Li, M.: The association of chemical composition particularly the heavy metals with the oxidative potential of ambient $PM_{2.5}$ in a megacity (Guangzhou) of southern China, Environ. Res., 213, 113489, 10.1016/j.envres.2022.113489, 2022c.

Yuan, W., Huang, R.-J., Luo, C., Yang, L., Cao, W., Guo, J., and Yang, H.: Measurement report: Oxidation potential of water-soluble aerosol components in the southern and northern of Beijing, Zenodo [data set], https://doi.org/10.5281/zenodo.10791126, 2024.

Yuan, W., Huang, R.-J., Yang, L., Guo, J., Chen, Z., Duan, J., Wang, T., Ni, H., Han, Y., Li, Y., Chen, Q., Chen, Y., Hoffmann, T., and O'Dowd, C.: Characterization of the light-absorbing properties, chromophore composition and sources of brown carbon aerosol in Xi'an, northwestern China, Atmos. Chem. Phys., 20, 5129-5144, 10.5194/acp-20-5129-2020, 2020.

Zhang, Q., Ma, H., Li, J., Jiang, H., Chen, W., Wan, C., Jiang, B., Dong, G., Zeng, X., Chen, D., Lu, S., You, J., Yu, Z., Wang, X., and Zhang, G.: Nitroaromatic Compounds from Secondary Nitrate Formation and Biomass Burning Are Major Proinflammatory Components in Organic Aerosols in Guangzhou: A Bioassay Combining High-Resolution Mass Spectrometry Analysis, Environ. Sci. Technol., 57, 21570-21580, https://doi.org/10.1021/acs.est.3c04983, 2023.
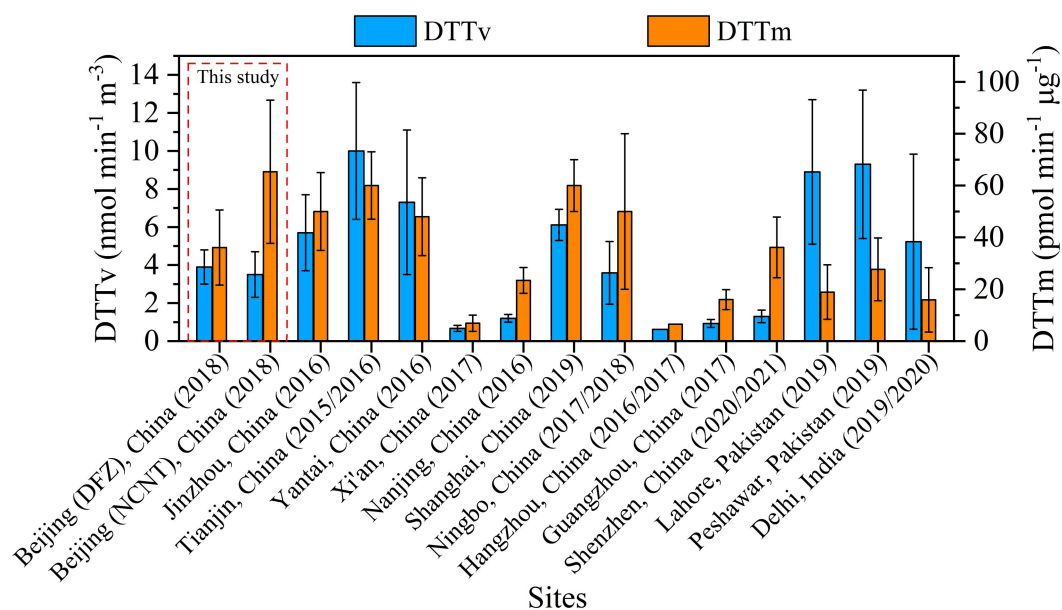
Zheng, Y., Davis, S. J., Persad, G. G., and Caldeira, K.: Climate effects of aerosols reduce economic inequality, Nat. Clim. Chang., 10, 220-224, 2020.

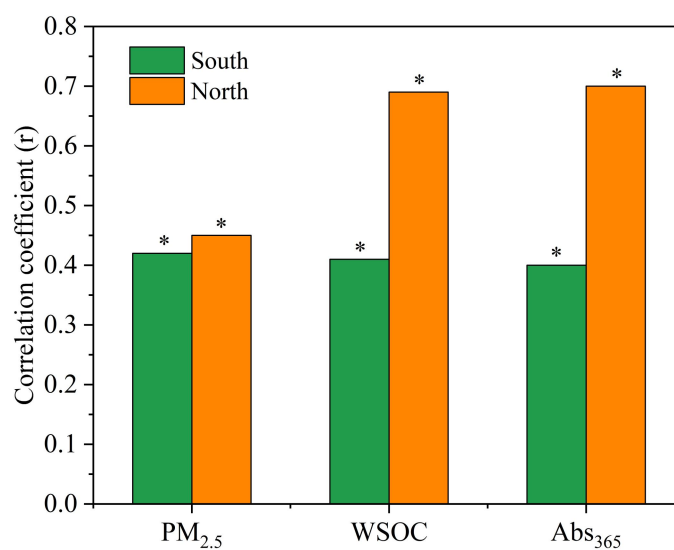804
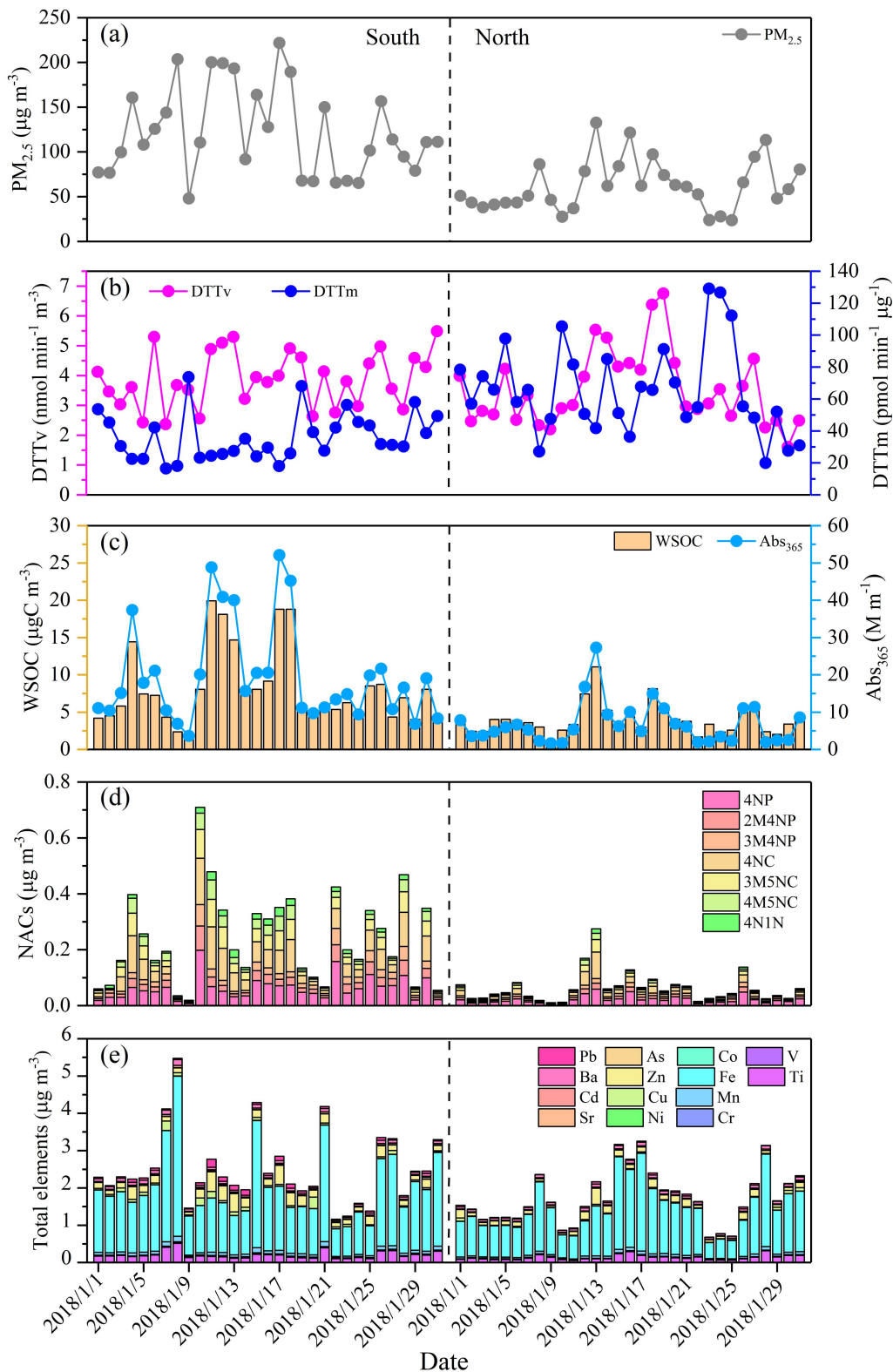
Figure 1. Time series of (a) $PM_{2.5}$ concentration, (b) DTT_v and DTT_m, (c) concentration and light absorption at wavelength 365 nm (Abs_{365}) of WSOC, concentrations of (d) NACs and (e) total elements.

Figure 2. Comparison of DTT_v and DTT_m values of water-soluble $PM_{2.5}$ measured in this study with those measured in other areas of Asia during similar period.
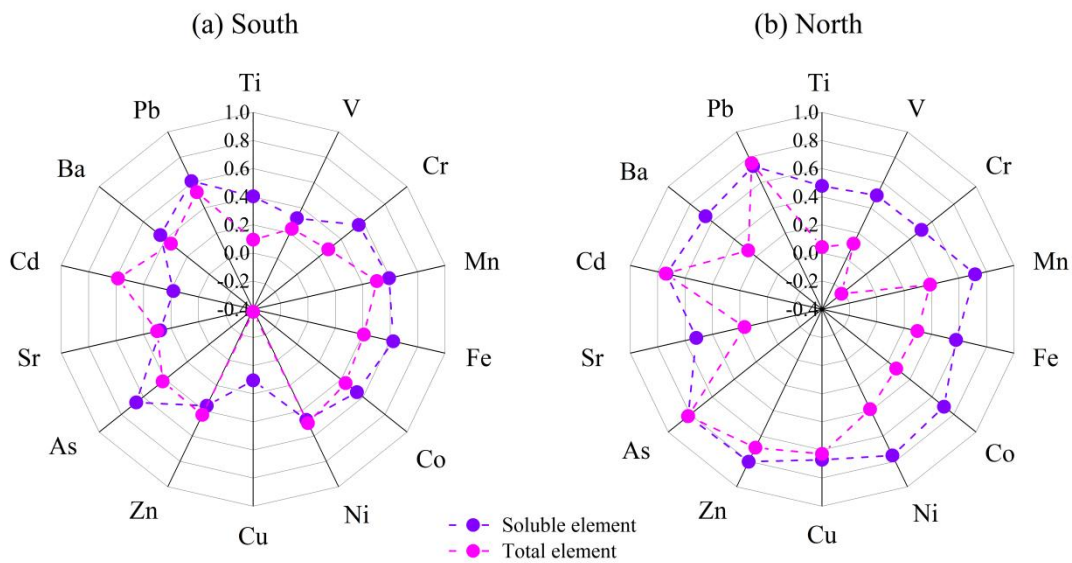

Figure 3. Correlation coefficients between DTT_v and $PM_{2.5}$, WSOC, and Abs_{365} in the south and north of Beijing (* indicates correlation is significant at the 0.05 level).
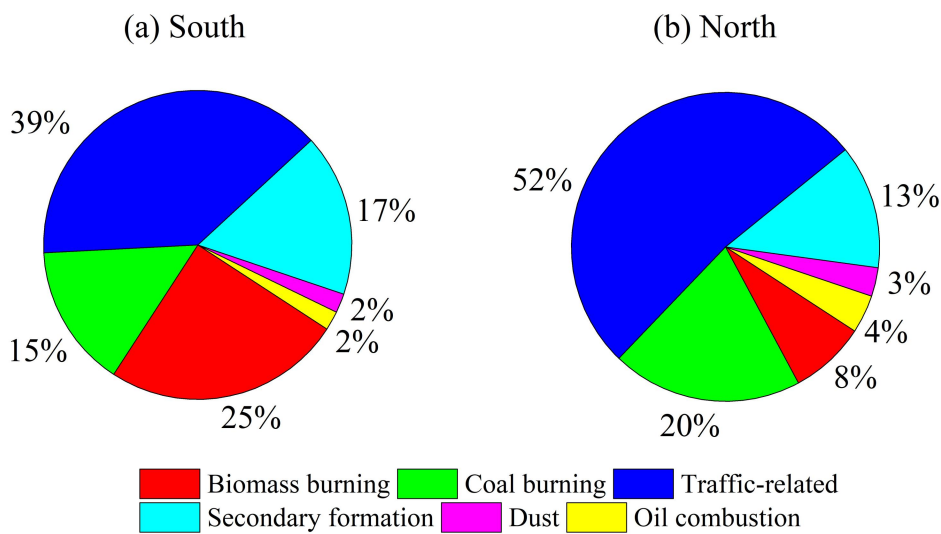
Figure 4. Correlation coefficients between DTT_v and elements in the (a) south and (b) north of Beijing.

Figure 5. Contributions of resolved sources to DTT_v in the (a) south and (b) north of Beijing.

31